



## Effect of thermophoresis on the motion of aerosol particles in natural convective flow on horizontal plates



Abhijit Guha, Subho Samanta\*

Mechanical Engineering Department, Indian Institute of Technology Kharagpur, Kharagpur 721302, India

### ARTICLE INFO

#### Article history:

Received 2 May 2013

Received in revised form 5 August 2013

Accepted 19 August 2013

#### Keywords:

Particle deposition  
Micro and nano particles  
Natural convection  
Brownian diffusion  
Thermophoresis  
Magnetohydrodynamics

### ABSTRACT

The present work investigates the effects of thermophoresis and transverse magnetic field on aerosol particle transport and deposition onto a horizontal plate in the presence of a natural convective flow. Micro to nano sized particles (particle diameter in the range 1 nm–1  $\mu$ m) are considered. A similarity solution for the fluid flow field is formulated for natural convection with and without magnetohydrodynamic (MHD) effects above a heated horizontal plate as well as beneath a cold horizontal plate. The mechanisms of particle deposition include the effects of free convection, Brownian diffusion and thermophoresis. Numerical results for the velocity and temperature fields of the fluid, and, the concentration profile and the deposition velocity of the particles are obtained and presented graphically as a function of pertinent parameters. The importance of Cunningham correction on the concentration profile and deposition velocity of ultrafine (sub-micron to nanometer) particles is demonstrated. It is found that the thicknesses of both the hydrodynamic boundary layer and thermal boundary layer increase with an increase in magnetic field parameter. The deposition velocity decreases with an increase in particle diameter  $d_p$  (i.e. an increase in particle Schmidt number  $Sc$ ), usually decreases with an increase in magnetic field parameter  $\zeta$ , and increases with an increase in the value of the coefficient of diffusion due to temperature gradient  $D_T$ . It is shown that for the cold plate facing downward, the thermal drift of particles assists Brownian diffusion. For the heated plate facing upward, the thermal drift away from the surface decreases the overall deposition velocity which decreases drastically above a certain particle size.

© 2013 Elsevier Ltd. All rights reserved.

### 1. Introduction

In the present paper, transport and deposition of small particles are analyzed for a natural convective boundary layer on a horizontal plate with or without magnetohydrodynamic effects. Natural convection takes place if there is a temperature difference between the plate and the quiescent fluid. A laminar natural convective boundary layer forms on a semi-infinite plate (within a certain range of Grashof number) if either a hot plate faces upward or a cold plate faces downward. For small particles (in the diameter range 1 nm–1  $\mu$ m), the same temperature gradient that establishes the natural convection in the base fluid provides an additional force on the particles. The force due to a temperature gradient in the flow field is known as the thermophoretic force and the resulting transport of particles is called thermophoresis. Thus, unlike thermophoretic movement of particles in forced convection where the fluid flow field and the imposed temperature field can be independently varied, the thermophoretic movement of

particles in natural convection represents a coupled problem. Other than thermophoresis, the motion of small particles is caused by the fluid flow and Brownian diffusion. The analysis presented in this paper involves all three mechanisms of particle transport.

The computation of the fluid flow field involves two important aspects, the first being the complexity of computing natural convective boundary layer on a horizontal plate. Natural convection on a heated vertical plate is a well studied phenomenon and is covered in all textbooks on convection heat transfer. The literature on the analysis of natural convection on a horizontal plate is much more limited [1–3]. The natural convection boundary layer above a horizontal plate is formed indirectly because of an induced pressure gradient and thus it is termed as ‘indirect natural convection’ [4]. In the standard analysis of natural convection on a vertical plate, it is assumed that  $\partial p/\partial x = -\rho_\infty g$  and  $\partial p/\partial y = 0$ . On the other hand, the boundary layer on a horizontal plate due to natural convection is such that  $\partial p/\partial y \neq 0$  and  $\partial p/\partial x$  cannot be neglected inside the boundary layer (even when  $\partial p_\infty/\partial x$  is zero).

The second important aspect of the computation of the fluid flow field is an accurate accounting of the magnetohydrodynamic effects. Magnetohydrodynamics (MHD) refers to the study of mutual interaction of fluid flow with magnetic fields. The

\* Corresponding author.

E-mail addresses: [a.guha@mech.iitkgp.ernet.in](mailto:a.guha@mech.iitkgp.ernet.in) (A. Guha), [subhosamanta@iitkgp.ac.in](mailto:subhosamanta@iitkgp.ac.in) (S. Samanta).

**Nomenclature**

$B$	magnetic field strength		
$C_c$	Cunningham correction		
$d_p$	diameter of particles		
$D_B$	Brownian diffusivity (Eq. (8))		
$D_T$	coefficient of temperature-gradient-driven diffusion (Eq. (6))		
$f$	reduced stream function (Eq. (17))		
$g$	gravitational acceleration		
$Gr_x$	Grashof number defined as $Gr_x = \frac{g\beta(T_w - T_\infty)x^3}{\nu^2}$		
$h$	reduced pressure difference (Eq. (17))		
$J$	flux of particles		
$k$	Boltzmann constant		
$Kn$	Knudsen number ( $Kn \equiv l/d_p$ )		
$l$	mean free path of the surrounding gas		
$N$	concentration		
$p$	static pressure of the fluid		
$Pr$	Prandtl number		
$p_\infty$	static pressure in the undisturbed fluid		
$Sc$	Schmidt number		
$T$	static temperature of the fluid		
$T_\infty$	static temperature in the undisturbed fluid		
$\Delta\hat{T}$	non-dimensional temperature difference ( $\Delta\hat{T} = (T_w - T_\infty)/T_\infty$ )		
$u$	velocity component in the x direction		
$v$	velocity component in the y direction		
$V_d$	deposition velocity		
$x$	horizontal coordinate		
$y$	vertical coordinate		
		<b>Greek</b>	
		$\alpha$	thermal diffusivity
		$\beta$	coefficient of thermal expansion at the reference temperature
		$\eta$	similarity variable
		$\kappa$	thermophoretic force coefficient (Eq. (7))
		$\lambda$	thermal conductivity
		$\mu$	viscosity of fluid
		$\nu$	kinematic viscosity of fluid
		$\phi$	non-dimensional concentration (Eq. (17))
		$\psi$	stream function (Eq. (17))
		$\rho$	density of fluid
		$\theta$	non-dimensional temperature (Eq. (17))
		$\zeta$	non-dimensional number used to specify the magnetic field strength ( $\zeta = \frac{\sigma B^2 x^2}{\mu (Gr_x)^{2/3}}$ )
			<b>Subscripts</b>
		$f$	fluid
		$p$	particle
		$w$	condition at the wall
		$\infty$	condition in undisturbed fluid
			<b>Superscripts</b>
		'	differentiation with respect to $\eta$
		$\wedge$	non-dimensional

phenomenon is a subject-matter of intensive research due to its diverse applications [5]. The analysis of laminar magnetohydrodynamic free convection flow of a viscous incompressible fluid past an impermeable semi-infinite horizontal plate with uniform surface temperature can be found in [6–8].

The effect of thermophoresis is included in the unified advection–diffusion theory of particle transport and deposition in laminar as well as turbulent flow (forced convection) developed by Guha [9–11]. Thermophoretic particle deposition in natural convective flow on a vertical plate has been studied by Epstein et al. [12] and Nazaroff and Cass [13] among others. In a recent study, Alam et al. [14] considered the effects of heat generation and thermophoresis in steady laminar hydromagnetic free convection flow over an inclined plate. However an examination of the governing equations presented in [14] reveals that they are not valid for a horizontal flat plate. It is believed that the present paper would be the first study of particle transport and deposition in natural convective flow on a horizontal plate, whether with or without MHD effects. Natural convection above a heated horizontal plate as well as that beneath a cold horizontal plate has been considered. The effects of magnetic field parameter ( $\zeta$ ), Schmidt number ( $Sc$ ) and nondimensional temperature ( $\Delta\hat{T}$ ) on particle transport and deposition are analyzed.

## 2. Mathematical formulation

Consider steady, laminar natural convection flow of a viscous and incompressible fluid past a semi-infinite horizontal plate. The plate is subjected to a constant wall temperature  $T_w$ . The free stream temperature and concentration are uniform and given by  $T_\infty$  and  $N_\infty$  respectively.

For mathematical modeling of aerosol particle flow due to natural convection past a semi-infinite horizontal plate, following assumptions are made:

- The flow of fluid is two dimensional in nature. The fluid can be assumed to be a continuum.
- Newton's law of linear relationship between shear stress and shear strain rate, and Fourier's law of heat diffusion are valid.
- The fluid is electrically conducting (for cases with magnetohydrodynamic effects).
- Viscous dissipation term in the energy equation is negligible. Hall effects and Joule heating are neglected.
- There is no internal energy generation.
- Transport parameters, like coefficient of thermal diffusivity, kinematic viscosity do not change with time and space, and density variation is also neglected, except in the body force term of momentum transport equation. Boussinesq approximation for density is assumed.
- Walls of the plate are impermeable.
- The magnetic Reynolds number is very small and hence induced magnetic field may be neglected.
- The particle concentration is dilute with zero particle concentration at the wall surface. All particles are of the same size and the particle size is small (diameter less than 1  $\mu\text{m}$ ). The particles are not charged. Effects of any body force (including gravity) on the particles are not considered.

Under the above assumptions the mass, momentum, energy and particle concentration equations in dimensional form are given by:

Continuity equation:

$$\frac{\partial u}{\partial x} + \frac{\partial v}{\partial y} = 0 \quad (1)$$

x-momentum equation:

$$u \frac{\partial u}{\partial x} + v \frac{\partial u}{\partial y} = -\frac{1}{\rho} \frac{\partial p}{\partial x} + \nu \frac{\partial^2 u}{\partial y^2} - \sigma \frac{B^2}{\rho} u \quad (2)$$

y-momentum equation:

$$-\frac{1}{\rho} \frac{\partial p}{\partial y} + g\beta(T - T_\infty) = 0 \tag{3}$$

Energy equation:

$$u \frac{\partial T}{\partial x} + v \frac{\partial T}{\partial y} = \alpha \frac{\partial^2 T}{\partial y^2} \tag{4}$$

Particle concentration equation:

$$u \frac{\partial N}{\partial x} + v \frac{\partial N}{\partial y} = D_B \frac{\partial^2 N}{\partial y^2} + D_T \frac{\partial}{\partial y} \left( \frac{1}{T} \frac{\partial T}{\partial y} N \right) \tag{5}$$

Guha [9–11] has derived generalized equations for particle transport and deposition from fundamental conservation laws. The equations are valid for laminar to turbulent flow, and, for wide range of particle size (nanoparticles to large millimeter-sized particles). The theory includes the effects of inertia, Brownian diffusion, thermophoresis, turbophoresis, electrical and other body forces, gravity, shear-induced lift, surface roughness, and corrections due to Knudsen effect or finite slip Reynolds number. These equations reduce to the well known relations in the appropriate limits. Thus, for example, Fick’s law of diffusion or the currently popular equations for the motion of nanoparticles can be viewed as subsets of the unified advection–diffusion theory derived. Experiments show that the deposition velocity varies differently with the size of particle in different ranges of particle size and it can vary by several orders of magnitude as particle size is altered. In the past, separate theories were needed in different particle size ranges and it would have been difficult to apply the theories to flow situations that are different from the situations for which the parameters of the theories were tuned. The unified advection–diffusion theory thus settles the quest over previous fifty years in the field for a physics-based explanation for the observed complex behaviour of particle transport. The present version of particle concentration Eq. (5) is a special case of the generalized particle transport equation. Only two terms representing Brownian diffusion and thermophoresis are retained in the RHS of Eq. (5). Since only laminar natural convection is considered here, the terms arising out of the interaction of the particle and fluid turbulence are not retained. Fluid velocities (instead of separate particle velocities) are used in the LHS of Eq. (5), this implies that the equation would be valid only for the transport of small particles (diameter less than 1 μm). It is assumed that there are no body forces acting on the particles, thus gravitational settling, and the effects of electrical or magnetic forces are not included in the present study.

Here  $x$  and  $y$  are dimensional coordinates along and normal to the plate,  $u$  and  $v$  are the velocity components in the  $x$  and  $y$  directions,  $p$  is the static pressure,  $g$  is the gravitational acceleration (only magnitude is to be considered since the sign is incorporated in the analysis),  $\beta$  is the coefficient of thermal expansion at the reference temperature,  $T_\infty$  is the ambient temperature,  $\rho, \nu$  and  $\alpha$  are the density, kinematic viscosity, and thermal diffusivity of the fluid respectively, and  $D_B$  is the Brownian diffusivity.  $D_T$  represents the coefficient of diffusion due to temperature gradient and is given by

$$D_T = D_B(1 + \kappa/kT) \tag{6}$$

Eq. (6), mathematically derived by Guha [9], shows that the thermal drift has a stressphoretic component and a thermophoretic component (the term containing  $\kappa$ ). The thermophoretic force coefficient,  $\kappa$ , is given by [15]

$$\kappa = \frac{2.34(6\pi\mu\nu r)(\lambda_r + 4.36Kn)}{(1 + 6.84Kn)(1 + 8.72Kn + 2\lambda_r)} \tag{7}$$

where  $\lambda_r$  is the ratio of the thermal conductivity of the fluid,  $\lambda$ , and that of the particles,  $\lambda_p$  ( $\lambda_r = \lambda/\lambda_p$ ). The thermophoretic force may be

significant for smaller particles even in the presence of a modest temperature gradient [9].

The Brownian diffusivity  $D_B$  in Eqs. (5) and (6) is calculated by Einstein’s relation modified by the Cunningham correction factor  $C_C$  to take account of the special situation arising at high Knudsen number  $Kn$  when the particle diameter is small [9]:

$$D_B = \left( \frac{kT}{3\pi\mu d_p} \right) C_C \tag{8}$$

There are a number of expressions for  $C_C$  available in the literature. Guha [11] has given two of the most used expressions for  $C_C$  as follows:

$$C_C = 1 + 2.7Kn \tag{9}$$

$$C_C = 1 + Kn[2.514 + 0.8 \exp(-0.55/Kn)] \tag{10}$$

Since the example calculations are presented in the particle diameter range 1 nm–1 μm, three separate computations are performed for each combination of particle size and other parameters corresponding to (i)  $C_C$  given by Eq. (9), (ii)  $C_C$  given by Eq. (10), and (iii)  $C_C = 1$  (i.e. with no Cunningham correction), in order to assess the importance of  $C_C$  on the natural convective motion of very small particles.

The boundary conditions for the solution of Eqs. (1)–(5) are:

$$\begin{aligned} \text{at } y = 0, \quad & u = 0, \quad v = 0, \quad T = T_w, \quad N = 0; \\ \text{at } y \rightarrow \infty, \quad & u \rightarrow 0, \quad p \rightarrow p_\infty, \quad T \rightarrow T_\infty, \quad N \rightarrow N_\infty. \end{aligned} \tag{11}$$

We introduce a stream function  $\psi$  defined by

$$u = \frac{\partial \psi}{\partial y} \text{ and } v = -\frac{\partial \psi}{\partial x} \tag{12}$$

which automatically satisfies the continuity Eq. (1).

We are then left with the following four equations

$$\frac{\partial \psi}{\partial y} \frac{\partial^2 \psi}{\partial x \partial y} - \frac{\partial \psi}{\partial x} \frac{\partial^2 \psi}{\partial y^2} = -\frac{1}{\rho} \frac{\partial p}{\partial x} + \nu \frac{\partial^3 \psi}{\partial y^3} - \sigma \frac{B^2}{\rho} \frac{\partial \psi}{\partial y} \tag{13}$$

$$-\frac{1}{\rho} \frac{\partial p}{\partial y} + g\beta(T - T_\infty) = 0 \tag{14}$$

$$\frac{\partial \psi}{\partial y} \frac{\partial T}{\partial x} - \frac{\partial \psi}{\partial x} \frac{\partial T}{\partial y} = \alpha \frac{\partial^2 T}{\partial y^2} \tag{15}$$

$$\frac{\partial \psi}{\partial y} \frac{\partial N}{\partial x} - \frac{\partial \psi}{\partial x} \frac{\partial N}{\partial y} = D_B \frac{\partial^2 N}{\partial y^2} + D_T \frac{\partial}{\partial y} \left( \frac{1}{T} \frac{\partial T}{\partial y} N \right) \tag{16}$$

We now introduce the following transformations:

$$\begin{aligned} \psi &= \nu(Gr_x)^{1/5} f(\eta), \quad B = B_0 x^{-2/5}, \quad (p - p_\infty) = \rho \frac{\nu^2}{x^2} (Gr_x)^{4/5} h(\eta), \\ \theta(\eta) &= \frac{T - T_\infty}{T_w - T_\infty}, \quad \phi(\eta) = \frac{N}{N_\infty} \end{aligned} \tag{17}$$

where the similarity variable  $\eta$  is defined as  $\eta = \frac{y}{x} (Gr_x)^{1/5}$  and  $Gr_x = \frac{g\beta(T_w - T_\infty)x^3}{\nu^2}$  is the local Grashof number.

Then, on substitution in Eqs. (13)–(16), we obtain the following sets of ordinary differential equations

$$f''' + \frac{3}{5}ff'' - \frac{1}{5}f'^2 + \frac{2}{5}\eta h' - \frac{2}{5}h - \zeta f' = 0 \tag{18}$$

$$h' = 0 \tag{19}$$

$$\frac{1}{Pr} \theta'' + \frac{3}{5}f\theta' = 0 \tag{20}$$

$$\frac{1}{Sc} \phi'' + \frac{3}{5}f\phi' + \left( \frac{D_T}{\nu} \right) \frac{\Delta \hat{T}}{1 + \Delta \hat{T} \theta} \left( \theta' \phi + \theta' \phi' - \frac{\Delta \hat{T}}{1 + \Delta \hat{T} \theta} \theta'^2 \phi \right) = 0 \tag{21}$$

where  $\zeta = \frac{\sigma B^2 x^2}{\mu (Gr_x)^{2/5}}$  represents the magnetic field parameter (square of the Hartmann number),  $B$  represents the strength of the applied magnetic field,  $Sc = \nu/D_B$  is the Schmidt number, and  $\Delta\hat{T} = (T_w - T_\infty)/T_\infty$  is the non-dimensional temperature difference. For  $T_\infty = 300$  K and  $(T_w - T_\infty) = 30$  K,  $\Delta\hat{T}$  corresponds to an approximate value of 0.1. A positive value of  $\Delta\hat{T}$  implies that the heated plate faces upward; a negative  $\Delta\hat{T}$  indicates that the cold plate faces downward.

It is important to mention in this regard that the condition  $B = B_0 x^{-2/5}$  ensures that the magnetic field parameter  $\zeta$  is independent of the distance  $x$ . One can anticipate the fact that when  $B \sim x^{-2/5}$ , there is a singular point at  $x = 0$  (i.e. at the leading edge of the plate). However, the boundary layer equations are not valid there any way.

Eqs. (18)–(21) are solved subject to the following boundary conditions

$$\begin{aligned} \text{at } \eta = 0, \quad f = 0, \quad f' = 0, \quad \theta = 1, \quad \phi = 0; \\ \text{at } \eta \rightarrow \infty, \quad f' \rightarrow 0, \quad h \rightarrow 0, \quad \theta \rightarrow 0, \quad \phi \rightarrow 1. \end{aligned} \quad (22)$$

The condition  $\phi = 0$  at  $\eta = 0$  is used as the boundary condition to reflect the perfectly absorbing characteristics of the surface. This is a reasonable assumption for small particles. It is possible to include more complex boundary condition derivable from the kinetic theory.

### 2.1. Orientation of the surface

The above analysis is performed for the natural convective boundary layer flow above a heated plate. It is found that the same governing equations and solutions would be valid for the natural convective flow beneath a cold plate, if the  $y$ -axis is chosen as positive downward for this case and the local Grashof number is defined as  $Gr_x = \frac{g\beta(T_\infty - T_w)x^3}{\nu^2}$ . Therefore, to keep the present analysis valid for both heated and cold plates, the Grashof number is generically defined as  $Gr_x = \frac{g\beta|T_w - T_\infty|x^3}{\nu^2}$ . The non-dimensional temperature difference  $\Delta\hat{T} = (T_w - T_\infty)/T_\infty$  is positive for the flow above a heated plate and negative for the flow beneath a cold plate. The appropriate sign of  $\Delta\hat{T}$  is reflected in the particle transport Eq. (21).

### 2.2. Natural convection without MHD effects

In the limit  $\zeta \rightarrow 0$ , Eqs. (18)–(20) reduce to those for laminar free convection above an isothermal horizontal plate without MHD effects. The solutions of these equations for different Prandtl number are thoroughly discussed in Reference [3]. Although the fluid flow field is given in [3], the computation of the motion of small particles in such flow field has not been performed previously. Thus the solutions of the particle equation (Eq. (21)) given in the present paper for  $\zeta \rightarrow 0$  are all new. These solutions of particle motion are of scientific importance, and are characteristically distinct from existing solutions of particle motion in forced convection with thermophoresis (i.e. with an imposed temperature gradient). This is so because, in natural convection, the effects of thermophoresis and fluid flow field on the motion of particles are inextricably linked with each other; the fluid flow field also depends on the same temperature difference between the surface and the free stream that determines the thermal drift of the particles. However, like the forced convection case, we wanted to determine the contribution of thermal drift on the overall motion of particles in the natural convection flow field. Note that one should not switch off the contribution of thermal drift alone by setting  $\Delta\hat{T} = 0$  in Eq. (21) since that would give rise to an inconsistent formulation ( $\Delta\hat{T} = 0$  would simultaneously mean that there is no natural convection). In the present study, we have therefore isolated the effects of thermal drift by artificially setting  $D_T = 0$  in

Eq. (21), these solutions are included in some of the graphs given later. Since one objective of the present paper is to extend the computations to ultrafine particles (particle diameter of the order of 1 nm), the Cunningham correction factor has been applied to the Brownian diffusivity term and three different expressions for the Cunningham correction factor have been examined to assess the sensitivity of the computed particle deposition velocity.

### 2.3. Stability analysis

It is possible to study the characteristics of vortex stability in magnetohydrodynamic natural convection flow over isothermal horizontal plates. Such analysis provides theoretical limits of Grashof number beyond which the assumption of a laminar boundary layer would not be valid. There are also engineering implications of the study of vortex stability in natural convection flow over a heated isothermal plate because of its industrial applications in chemical vapor deposition process and the cooling of electronic packages. The presence of vortices can lead to nonuniform deposition in chemical vapor deposition processes. On the other hand, it is desirable to enhance vortex flow to increase heat transfer from a surface [16]. The fact that in natural convection on horizontal plates the buoyancy force acts perpendicular to the plate is responsible for causing the instability. The stability of flow in laminar natural convection above an isothermal horizontal plate (without magnetohydrodynamic effect) has been studied by a few researchers [17,18]. The critical Grashof number ( $Gr_x^*$ ) which marks the onset of vortex instability can be found from the minima of the neutral stability curve. Jang [17] considered linear stability using parallel flow model but the values of critical Grashof number obtained from such analysis are two orders lower in magnitude in comparison to the experimental results of Cheng and Kim [19]. This is because the parallel flow model disregards the streamwise growth of boundary layer. However, the nonparallel flow analysis considered in [18] provides a larger critical Grashof number than the parallel flow model, thus showing better agreement with the experimental results of Cheng and Kim [19]. The above-mentioned trend for natural convection is also true for the case of Blasius boundary layer flow. The value of critical Reynolds number obtained from linear stability analysis using parallel flow model for Blasius boundary layer is 520 whereas experiments show that the transition to turbulence occurs beyond a Reynolds number of  $10^5$  [20].

Leu and Jang [21] considered hydrodynamic stability of laminar natural convection flow over an isothermal horizontal plate in the presence of a transverse magnetic field. The base flow equations considered in their study are identical to the Eqs. (18)–(20) used in the present analysis. They performed a linear stability analysis using parallel flow model and found that the presence of a transverse magnetic field destabilizes the flow and marks an early onset of instability. It was shown in [21] that the value of the critical Grashof number ( $Gr_x^*$ ) decreases drastically as the magnetic field parameter  $\zeta$  is increased from 0 to 4. However the nonparallel flow model considered by Chen [16] shows that the critical Grashof number in natural convection boundary layer flow above an isothermal horizontal plate is almost unaffected by the presence of a transverse magnetic field of small strength ( $0 \leq \zeta \leq 5$ ). For  $\zeta = 0$ , the linear stability analysis using nonparallel flow model [16,18] provides the value of critical Grashof number that is of the same order of magnitude as found in experiments of Cheng and Kim [19]. It is to be mentioned in this regard that the experimentally measured value of critical Grashof number is  $8.86 \times 10^5$  with a standard deviation of  $2.51 \times 10^5$  for laminar natural convection above an isothermal horizontal plate in the absence of magnetic field [19].

2.4. Non-dimensional deposition velocity

The particle deposition flux to the wall surface can be determined using the definition

$$J_w = D_B \left( \frac{\partial N}{\partial y} \right)_{y=0} = D_B \left( \frac{N_\infty}{X} \right) (Gr_x)^{1/5} \phi'(0) \tag{23}$$

The deposition velocity is defined as the particle flux divided by the free stream concentration,

$$V_d = \frac{J_w}{N_\infty} = D_B X^{-1} (Gr_x)^{1/5} \phi'(0) \tag{24}$$

The local non-dimensional deposition velocity is defined as  $\widehat{V}_d = V_d X / \nu$ , so that

$$\widehat{V}_d = \frac{1}{Sc} \phi'(0) (Gr_x)^{1/5} \tag{25}$$

where  $\phi'(0)$  depends on  $\zeta$ ,  $Sc$ ,  $\Delta \hat{T}$  and  $D_T$  for a fixed  $Pr$ .

3. Method of solution

The system of Eqs. (18)–(21), subject to boundary conditions (22) has been solved numerically for various values of the magnetic field parameter ( $\zeta$ ), Schmidt number ( $Sc$ ) and coefficient of diffusion due to temperature gradient ( $D_T$ ) using the shooting method. The thermophysical properties of air are considered at a reference temperature of 300 K.  $\lambda_r$  is taken equal to 0.1 in all calculations.  $\zeta$  is varied from 0 to 5 throughout the computations. Schmidt number  $Sc$  is varied from 3.13 to  $6.04 \times 10^5$  which corresponds to particle diameter in the range of 0.001–1  $\mu\text{m}$ . The coefficient of diffusion due to temperature gradient ( $D_T$ ) varies from  $1.38 \times 10^{-5}$  to  $6.48 \times 10^{-6}$  in the range of particle diameter 0.001–1  $\mu\text{m}$ . Unless stated otherwise, the Cunningham correction used in all calculations is given by Eq. (10).

Eqs. (18)–(20) representing the interaction of fluid flow and heat transfer in laminar natural convection on horizontal surface are solved first; the particle continuity Eq. (21) is solved after the fluid flow field has been determined. Such sequential solution method is applicable because of the assumed one-way coupling between the fluid and the particles. The system of Eqs. (18)–(20) are first reduced to a set of six first order equations. The equations are then solved by marching forward in  $\eta$ . The boundary values of  $f(0)$ ,  $g(0)$  and  $h(0)$  are first guessed and these guessed values are updated in each iteration using the Newton method for simultaneous equations until agreement is reached with the prescribed conditions at  $\eta \rightarrow \infty$ . The far-field asymptotic value of  $\eta$  during the numerical computation is taken equal to 15 in order to ensure that the velocity and temperature profiles approach the ambient fluid conditions asymptotically. A truncated domain leads to errors in the values of wall shear stress and wall heat transfer. A knowledge of the converged velocity and temperature fields is required for the solution of particle continuity Eq. (21). After solving Eqs. (18)–(20), the particle continuity Eq. (21) is solved with a guessed value for  $\phi'(0)$ . The guessed value is updated in each iteration using Brent’s method. The value of  $\eta_\infty$  is varied from 5 to 15 depending on the particle Schmidt number ( $Sc$ ) and magnetic field parameter  $\zeta$ . A very high value of  $\eta_\infty$  gives rise to an ill-conditioned matrix which presents numerical difficulty in attaining a converged solution. In the present computations, a solution is said to converge when the difference between the computed and specified boundary values at  $\eta \rightarrow \infty$  is less than  $10^{-6}$ . In order to make sure that the numerical solution is not significantly dependent on the step size a systematic study has been carried out with step sizes equal to 0.001, 0.01 and 0.05. It has been found that the values of  $f'(0)$ ,  $-\theta'(0)$  and  $\phi'(0)$  do not change up to five decimal places for step size

Table 1 Comparison of the values of  $f'(0)$  and  $-\theta'(0)$  for  $Pr = 0.72$  and  $\zeta = 0$ .

	Present similarity solution	Rotem and Claassen [1]	Chen et al. [2]
$f'(0)$	0.9784	0.9799	0.9791
$-\theta'(0)$	0.3574	0.3590	0.3582

values corresponding to 0.001 and 0.01. A fourth-order Runge–Kutta method with step size of 0.01 was chosen for the integration of differential equations.

In the absence of magnetic field and particle transport, the present Eqs. (18)–(20) subject to boundary conditions (22) reduce to the classical problem of laminar natural convection over a horizontal plate as presented in Rotem and Claassen [1]. To check the validity of the present code, the longitudinal velocity  $f(\eta)$  and non-dimensional temperature  $\theta(\eta)$  is plotted as a function of  $\eta$  for  $Pr = 0.72$  in the absence of magnetic field. The plotted graphs show excellent agreement with the results of Rotem and Claassen [1] and Chen et al. [2] and, hence, act as a validation of the developed computational scheme. Table 1 presents a comparison of the values of  $f'(0)$  and  $\theta'(0)$  produced by the present code and that of Rotem and Claassen [1] and Chen et al. [2]. It is observed that the results agree well with the previously published results.

4. Results and discussion

Since the mechanisms of particle motion include Brownian diffusion, convection effects caused by fluid motion and thermophoresis caused by temperature gradient, it is necessary to discuss the fluid flow field and the temperature field first before analyzing the concentration distribution.

Fig. 1 shows the effect of magnetic field parameter  $\zeta$  on the longitudinal velocity profiles. From Eqs. (12) and (17), one can show that the longitudinal velocity in the  $x$  – direction is proportional to  $f(\eta)$  ( $\partial \psi / \partial y = \frac{\nu}{x} (Gr_x)^{2/5} f(\eta)$ ). The figure shows that at a particular value of  $\zeta$ ,  $f(\eta)$  initially increases with  $\eta$ , goes to a maximum and then decreases asymptotically to zero. The thickness of the momentum boundary layer increases with increase in  $\zeta$ , as can be seen from the figure. The velocity gradient at the surface of the plate is higher when the magnetic field parameter  $\zeta$  is small. The skin friction coefficient, which is proportional to  $f'(0)$ , decreases with an increase in  $\zeta$ . The presence of transverse magnetic field in an electrically conducting fluid introduces a damping effect on the velocity field by creating a drag force. This resistive force

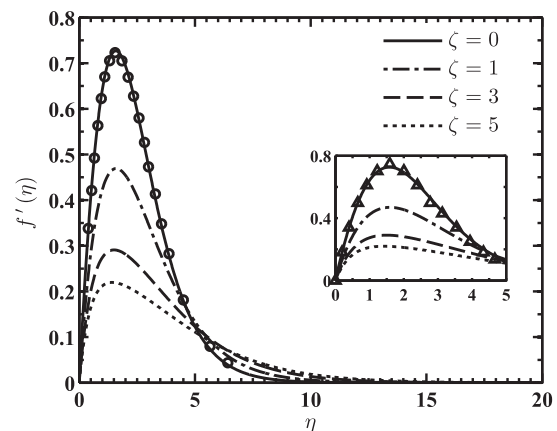


Fig. 1. Non-dimensional self-similar velocity profiles for an isothermal plate for various values of magnetic field parameter  $\zeta$  for  $Pr = 0.72$  (○ Similarity solution for  $\zeta = 0$  [1]; △ Numerical solution of integro-differential equations for  $\zeta = 0$  [2]).

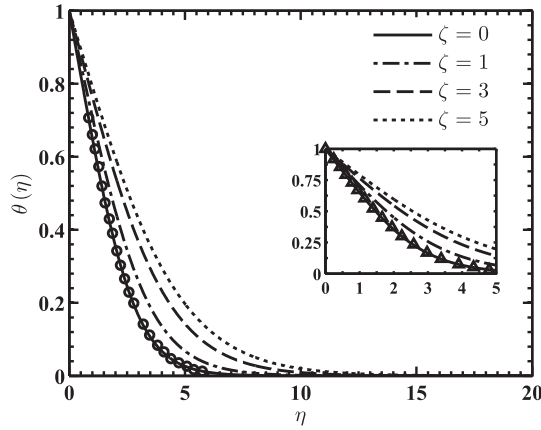


Fig. 2. Non-dimensional self-similar temperature profiles for an isothermal plate for various values of magnetic field parameter  $\zeta$  for  $Pr = 0.72$  ( $\circ$  Similarity solution for  $\zeta = 0$  [1];  $\Delta$  Numerical solution of integro-differential equations for  $\zeta = 0$  [2]).

causes the velocity to decrease with an increase in the magnetic field parameter  $\zeta$ . With increasing  $\zeta$ , the maximum velocity occurs at a smaller value of  $\eta$  as can be seen from the figure. An examination of Eq. (13) shows an interesting fact that the term containing the effect of the magnetic field depends on the square of the intensity of the magnetic field ( $B^2$ ). Hence, whatever is the direction of the magnetic field, the force is always resistive in nature.

Fig. 2 shows the effect of magnetic field parameter  $\zeta$  on the temperature profiles. From Eq. (17) it is observed that the non-dimensional fluid temperature is represented by  $\theta(\eta) = (T - T_\infty) / (T_w - T_\infty)$ . The figure shows that for a particular value of  $\zeta$ , at the surface of the plate ( $\eta = 0$ ) the fluid temperature is equal to the plate temperature ( $\theta(\eta)$  is unity). The fluid temperature asymptotically reaches the unperturbed value of temperature  $T_\infty$  ( $\theta(\eta)$  is 0) at large distance from the plate surface. The thickness of the thermal boundary layer increases with increase in magnetic field parameter  $\zeta$ . The application of magnetic field results in fluid deceleration which causes an increase in the temperature of the fluid close to the surface when a heated plate faces upward ( $\Delta\hat{T}$  is positive) or a decrease in the temperature of the fluid close to the surface when a cold plate faces downward ( $\Delta\hat{T}$  is negative). The surface heat flux, however, decreases with increasing  $\zeta$  for both positive and negative values of  $\Delta\hat{T}$ .

Fig. 3 presents the non-dimensional particle concentration profiles  $\phi(\eta)$  in the natural convection boundary layer adjacent to a horizontal flat plate for various values of particle diameter. From Eq. (17) it can be seen that the non-dimensional particle concentration is represented by  $\phi(\eta) = N/N_\infty$ . Fig. 3a presents the variation in  $\phi(\eta)$  for an upward facing heated horizontal plate. Fig. 3b presents the variation in  $\phi(\eta)$  for a downward facing cold horizontal plate. The thickness of the concentration boundary layer decreases with an increase in particle diameter ( $d_p$ ). An increase in particle diameter causes an increase in Schmidt number ( $Sc$ ) which represents the relative thicknesses of the velocity to concentration boundary layers. For a fluid with constant  $Pr$  and at a particular Grashof number  $Gr_x$ , the thickness of velocity boundary layer is fixed and thus an increase in value of  $Sc$  causes a decrease in the thickness of concentration boundary layer. From Fig. 3a it can be seen that for certain combinations of positive  $\Delta\hat{T}$  and large size of particles, thermophoresis drives the concentration boundary layer away to form a particle-free region close to the plate surface.

Fig. 4 depicts the influence of magnetic field parameter  $\zeta$  and  $\Delta\hat{T}$  on the particle concentration profiles  $\phi(\eta)$ . For the case of heated plate facing upwards ( $\Delta\hat{T} = 0.2$ ), the concentration gradient is smaller at the wall but the thickness of the concentration

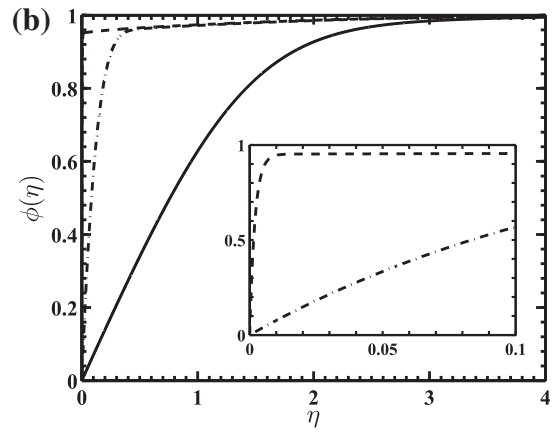
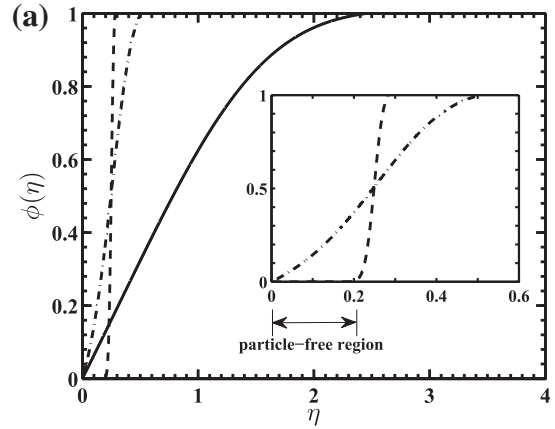


Fig. 3. Particle concentration profiles for an isothermal plate for various values of particle diameter  $d_p$  for  $\zeta = 0$  (a)  $\Delta\hat{T} = 0.1$ , (b)  $\Delta\hat{T} = -0.1$  (—  $d_p = 0.001 \mu\text{m}$ ; - - -  $d_p = 0.01 \mu\text{m}$ ; - · -  $d_p = 0.1 \mu\text{m}$ .  $\Delta\hat{T}$  is positive for flow above heated plate,  $\Delta\hat{T}$  is negative for flow beneath a cold plate.)

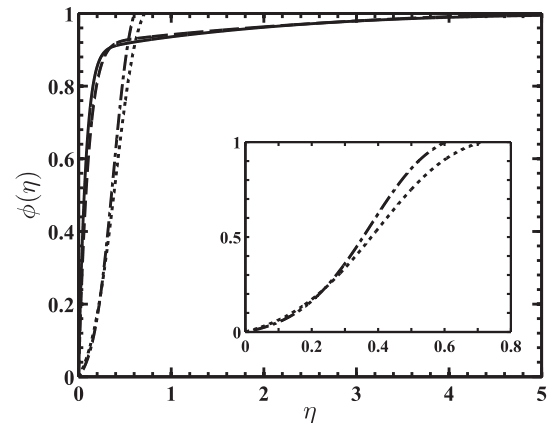


Fig. 4. Particle concentration profiles for an isothermal plate for various values of  $\zeta$  and  $\Delta\hat{T}$  (—  $\zeta = 1$ ,  $\Delta\hat{T} = -0.2$ ; - - -  $\zeta = 5$ ,  $\Delta\hat{T} = -0.2$ ; - · -  $\zeta = 1$ ,  $\Delta\hat{T} = 0.2$ ; ·····  $\zeta = 5$ ,  $\Delta\hat{T} = 0.2$ . For all curves,  $d_p = 0.01 \mu\text{m}$ .  $\Delta\hat{T}$  is positive for flow above heated plate,  $\Delta\hat{T}$  is negative for flow beneath a cold plate.)

boundary layer is also smaller as compared to the case of a cold plate facing downwards ( $\Delta\hat{T} = -0.2$ ). It is found that the particle concentration gradient at the surface of the plate depends weakly on the magnetic field parameter  $\zeta$ . This has implication on the deposition velocity (to be discussed later in connection with Fig. 6).

The effect of non-dimensional temperature difference  $\Delta\hat{T}$  on the particle concentration profiles  $\phi(\eta)$  is portrayed in Fig. 5. For the

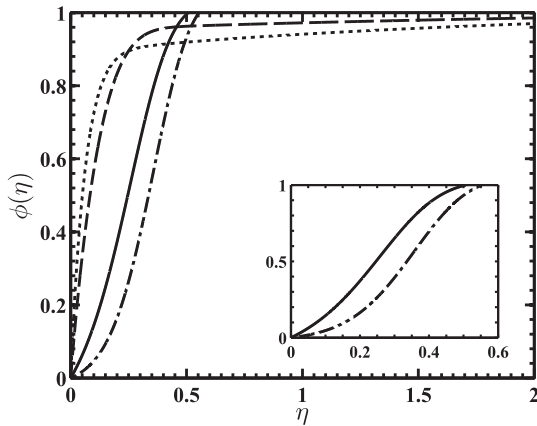


Fig. 5. Particle concentration profiles for an isothermal plate for various values of  $\Delta\hat{T}$  for  $\zeta=0$  and  $d_p=0.01\ \mu\text{m}$  (—  $\Delta\hat{T}=0.1$ ; - - -  $\Delta\hat{T}=0.2$ ; - - -  $\Delta\hat{T}=-0.1$ ; .....  $\Delta\hat{T}=-0.2$ .  $\Delta\hat{T}$  is positive for flow above heated plate,  $\Delta\hat{T}$  is negative for flow beneath a cold plate.)

parametric conditions used in the figure, it can be seen that an increase in non-dimensional temperature difference  $\Delta\hat{T}$  (from  $-0.2$  to  $0.2$ ) decreases the concentration gradient at the surface of the plate  $\phi'(0)$ . For a heated plate facing upwards,  $\Delta\hat{T}$  is positive. The second derivative of concentration profile  $\phi''$  is positive at the surface of the plate whereas it is negative close to the edge of the boundary layer. Thus the concentration profile has a point of inflexion within the boundary layer and it takes a S-shape. For a cold plate facing downwards,  $\phi''$  is negative throughout the boundary layer and the particle concentration monotonically increases until it asymptotically reaches the unperturbed value  $N_\infty$  far away from the plate surface. This explains the fundamental difference in the shapes of the concentration profiles for negative and positive values of  $\Delta\hat{T}$ .

Fig. 6 presents the variation in non-dimensional deposition velocity ( $\hat{V}_d$ ) with magnetic field parameter ( $\zeta$ ) for an isothermal plate. Fig. 6a shows the variation in deposition velocity ( $\hat{V}_d$ ) when a heated surface faces upwards (i.e. positive  $\Delta\hat{T}$ ). Fig. 6b shows the variation in deposition velocity ( $\hat{V}_d$ ) when a cold surface faces downwards (i.e. negative  $\Delta\hat{T}$ ). For the cold plate, the deposition velocity decreases with an increase in magnetic field parameter ( $\zeta$ ) for all sizes of the particles. For an upward facing heated horizontal plate, the deposition velocity decreases with an increase in  $\zeta$  when the particle size is small, but the deposition velocity increases when the particle size is large. The physical explanation for the above trends is intricate in nature. The datum trend in the variation of deposition velocity with increasing  $\zeta$  for the effects of fluid convection and Brownian diffusion (i.e. without thermal drift) may be conceptualized by repeating all calculations shown in Fig. 6 with the imposed condition  $D_T=0$ . These calculations shown in Fig. 6c reveal that, for all particle sizes and for both positive as well as negative  $\Delta\hat{T}$ , the deposition velocity decreases slowly with increasing  $\zeta$ . Let us symbolically designate these results as RSO as a reference for the subsequent discussion. Any difference between the result set RSO and those shown in Fig. 6(a) and (b) is due to the effects of thermal drift. The nature of thermal drift is fully explained later in reference to Fig. 7. Here, we state a few essential facts that are necessary to understand Fig. 6. For a particle diameter of  $0.001\ \mu\text{m}$ , the effect of thermophoresis is negligible (as compared to the Brownian diffusion). This is why the curve for these particles shown in Fig. 6(a), that shown in Fig. 6(b) and the data of result set RSO show the same trend and are almost the same in magnitude. For the cold surface facing downward (i.e. negative  $\Delta\hat{T}$ ), thermophoresis enhances deposition velocity of larger

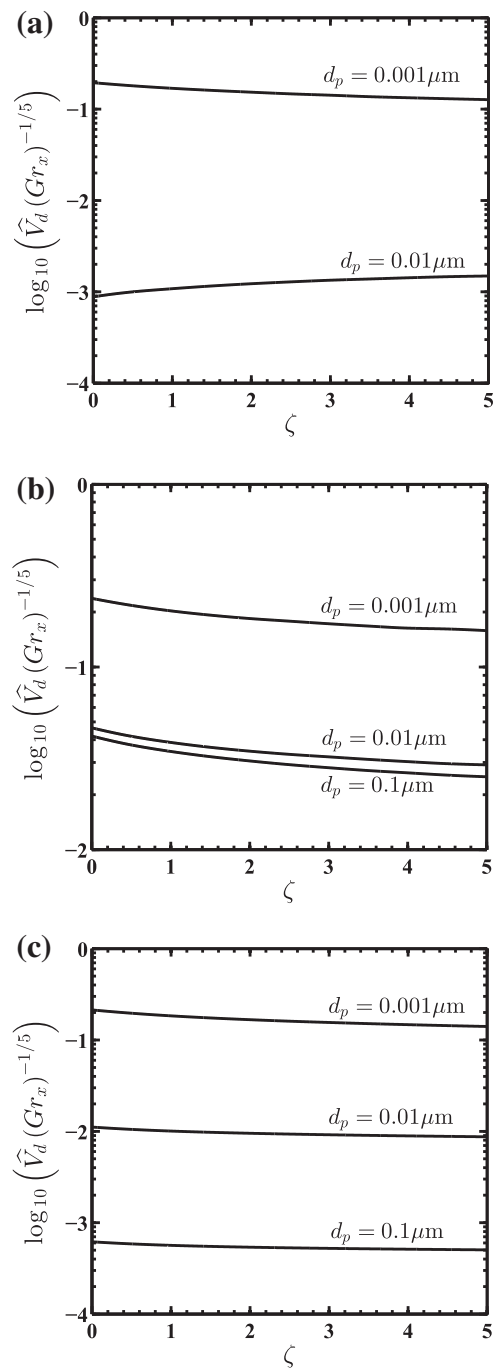
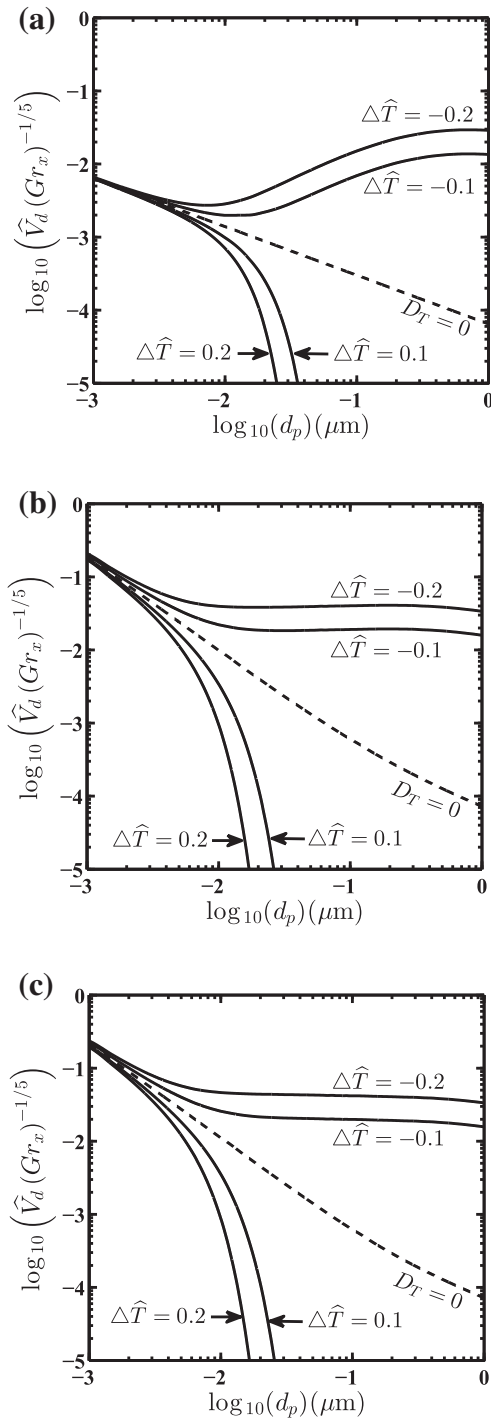


Fig. 6. Variation in non-dimensional deposition velocity ( $\hat{V}_d$ ) with magnetic field parameter  $\zeta$  for an isothermal plate (a)  $\Delta\hat{T}=0.2$ , (b)  $\Delta\hat{T}=-0.2$ , (c)  $D_T=0$ . ( $\Delta\hat{T}$  is positive for flow above heated plate,  $\Delta\hat{T}$  is negative for flow beneath a cold plate.)

particles, since both Brownian diffusion and thermophoresis act in the same direction. This is why the magnitude of deposition velocity shown in Fig. 6b is greater than the result set RSO, but the deposition velocity shown in Fig. 6(b) also decreases faster with increasing  $\zeta$  than RSO. The last aspect may be explained as follows. In connection with Fig. 2 it has been explained that an increase in  $\zeta$  decreases surface heat flux, i.e. decreases the magnitude of temperature gradient close to the surface. This decreases the thermophoretic movement of particles towards the cold surface. This additional effect increases the rate of decrease of the deposition velocity with increasing  $\zeta$  as compared to the



**Fig. 7.** Variation in non-dimensional deposition velocity ( $\widehat{V}_d$ ) with particle diameter  $d_p$  for an isothermal plate for  $\zeta=0$  (a)  $C_c=1$ , (b)  $C_c=1+2.7Kn$ , (c)  $C_c=1+Kn[2.514+0.8 \exp(-0.55/Kn)]$ . ( $\Delta\widehat{T}$  is positive for flow above heated plate,  $\Delta\widehat{T}$  is negative for flow beneath a cold plate.)

result set RS0. For the heated plate facing upward (i.e. positive  $\Delta\widehat{T}$ ), an increase in the magnetic field parameter  $\zeta$  again decreases the magnitude of the temperature gradient close to the surface. This decreases the thermophoretic movement of particles away from the plate. For a particle diameter of  $0.01 \mu\text{m}$ , the increase in deposition velocity (toward the surface) due to the decrease in thermophoretic component (away from the surface) more than offsets the decrease inherent in result set RS0. This is why for such combinations of particle size and  $\Delta\widehat{T}$ , the deposition velocity

increases with increasing  $\zeta$  as shown in Fig. 6(a). The trend for the variation of deposition velocity for a particle diameter of  $0.1 \mu\text{m}$  is similar to that for a particle diameter of  $0.01 \mu\text{m}$ , but the absolute values involved are several orders of magnitude lower and hence are not included in Fig. 6(a).

Fig. 7 presents the non-dimensional deposition velocity ( $\widehat{V}_d$ ) for particles of diameter  $0.001\text{--}1 \mu\text{m}$  as obtained from the numerical solution of particle concentration Eq. (21). Since Eq. (25) shows that  $\widehat{V}_d \propto (Gr_x)^{1/5}$ , the composite variable  $\widehat{V}_d (Gr_x)^{-1/5}$  is plotted as the ordinate in Fig. 7: in this way data generated by comprehensive computations can be presented in a concise manner. In order to assess the importance of the Cunningham correction on the motion of small particles, all computations are repeated with three different expressions for  $C_c$ . Fig. 7(a) presents the variation in local deposition velocity when  $C_c=1$ . Fig. 7b shows the variation in local deposition velocity when  $C_c$  is obtained from Eq. (9) whereas Fig. 7c is based on computations when  $C_c$  is obtained from Eq. (10). A comparison of the three figures show a significant difference in the predicted motion of small particles; for nanometer-sized particles the deposition velocity for  $C_c=1$  is more than one order of magnitude lower than that predicted for  $C_c$  given by Eq. (10). However, the deposition velocities obtained by using  $C_c$  from Eqs. (9) and (10) are almost identical.

When the Cunningham correction is incorporated, Fig. 7(b) and (c) show that the particle deposition velocity decreases with an increase in particle diameter at a particular Grashof number. With the Cunningham correction in place, both the Brownian diffusivity of particles ( $D_B$ ) and the coefficient of diffusion due to temperature gradient ( $D_T$ ) decrease with an increase in particle size. For the cold plate facing downward ( $\Delta\widehat{T}$  is negative), both Brownian diffusion and motion due to temperature gradient are towards the surface, hence these two effects assist each other to produce the overall deposition rate. When the particle size is very small (such as nanoparticles), the Brownian diffusion is the dominant mechanism. This is why the curves with various values of negative  $\Delta\widehat{T}$  approach one another for very small size of particles. As the particle size increases, both  $D_B$  and  $D_T$  decrease but the decrease in  $D_B$  is faster. This is why thermophoresis component assumes dominance for large particles. In this regime, the deposition velocity is greater for higher values of  $|\Delta\widehat{T}|$ , and the difference in the deposition velocity as compared to the hypothetical curve for  $D_T=0$  (giving zero thermophoresis) grows as the particle size increases. For the heated plate facing upward ( $\Delta\widehat{T}$  is positive), the particles tend to move towards the surface as a result of Brownian diffusion but tend to move away from the surface as a result of the temperature gradient. In this case, these two effects oppose each other to produce the overall deposition rate. Since  $D_T$  decreases at a lower rate than  $D_B$  with an increase in particle size, the effect of thermophoresis may dominate for large particles and the deposition velocity may decrease drastically. For a given value of  $\Delta\widehat{T}$ , there is a particle size above which virtually no particle is able to reach the surface. This is reflected as a particle-free region in the concentration profile, one example of which has been shown in Fig. 3(a).

## 5. Conclusions

The present work analyzes the effects of thermophoresis and transversely applied magnetic field on the concentration and motion of aerosol particles in steady laminar natural convection boundary layer flow on an isothermal horizontal plate. The particle transport mechanisms include viscous drag, Brownian diffusion, and thermophoresis. A similarity solution is formulated for the fluid flow field due to magnetohydrodynamic natural convection. The particle continuity equation is then solved to determine the concentration profile and non-dimensional deposition velocity on

the surface. Numerical results are presented to illustrate the effects of various governing parameters on the particle deposition velocity. Even in the absence of MHD effects, the present work represents the first study of particle motion due to natural convection on a horizontal plate.

It is found that the thicknesses of both the hydrodynamic boundary layer and thermal boundary layer increase with an increase in magnetic field parameter. The deposition velocity decreases with an increase in particle diameter  $d_p$  (i.e. an increase in particle Schmidt number  $Sc$ ), usually decreases with an increase in magnetic field parameter  $\zeta$ , and increases with an increase in the value of the coefficient of diffusion due to temperature gradient  $D_T$ . It is shown that an appropriate expression for the Cunningham correction must be included in the analysis since the concentration profile and deposition velocity of small particles depend strongly on the Cunningham correction.

The present work considers the natural convective boundary layer above a heated horizontal plate as well as that beneath a cold horizontal plate. It is shown that for the heated plate facing upward, the thermal drift away from the surface decreases the overall deposition velocity which decreases drastically above a certain particle size. For the cold plate facing downward, thermal drift of particles assists Brownian diffusion. The curve with  $D_T = 0$  is included in Fig. 7 to conceptually assess the importance of thermal drift on particle motion even though natural convective fluid flow field and thermal drift are inextricably linked through the same temperature difference between the horizontal plate and the quiescent fluid.

## References

- [1] Z. Rotem, L. Claassen, Natural convection above unconfined horizontal surfaces, *J. Fluid Mech.* 39 (1) (1969) 173–192.
- [2] T.S. Chen, H.C. Tien, B.F. Armaly, Natural convection on horizontal, inclined, and vertical plates with variable surface temperature or heat flux, *Int. J. Heat Mass Transfer* 29 (10) (1986) 1465–1478.
- [3] S. Samanta, A. Guha, A similarity theory for natural convection from a horizontal plate for prescribed heat flux or wall temperature, *Int. J. Heat Mass Transfer* 55 (13–14) (2012) 3857–3868.
- [4] H. Schlichting, K. Gersten, *Boundary-Layer Theory*, 8th ed., Springer, New Delhi, 2004.
- [5] P.A. Davidson, *An Introduction to Magneto-hydrodynamics*, 1st ed., Cambridge University Press, Cambridge, UK, 2001.
- [6] A.S. Gupta, Hydromagnetic free convection flows from a horizontal plate, *AIAA J.* 4 (8) (1966) 1439–1441.
- [7] P. Singh, Hydromagnetic free convection flow from a horizontal plate: Similar solution, *Acta Physica Academiae Scientiarum Hungaricae* 38 (2) (1975) 109–116.
- [8] S. Samanta, A. Guha, Magneto-hydrodynamic free convection flow above an isothermal horizontal plate, *Commun. Nonlinear Sci. Numer. Simul.* 18 (12) (2013) 3407–3422.
- [9] A. Guha, A unified Eulerian theory of turbulent deposition to smooth and rough surfaces, *J. Aerosol Sci.* 28 (8) (1997) 1517–1537.
- [10] A. Guha, A generalized mass transfer law unifying various particle transport mechanisms in dilute dispersions, *Heat Mass Transfer* 44 (11) (2008) 1289–1303.
- [11] A. Guha, Transport and deposition of particles in turbulent and laminar flow, *Ann. Rev. Fluid Mech.* 40 (2008) 311–341.
- [12] M. Epstein, G.M. Hauser, R.E. Henry, Thermophoretic deposition of particles in natural convection flow from a vertical plate, *J. Heat Transfer* 107 (2) (1985) 272–276.
- [13] W.W. Nazaroff, G.R. Cass, Particle deposition from a natural convection flow onto a vertical isothermal flat plate, *J. Aerosol Sci.* 18 (4) (1987) 445–455.
- [14] M.S. Alam, M.M. Rahman, M.A. Sattar, Similarity solutions for hydromagnetic free convective heat and mass transfer flow along a semi-infinite permeable inclined flat plate with heat generation and thermophoresis, *Nonlinear Anal.: Model. Control* 12 (4) (2007) 433–445.
- [15] L. Talbot, R.K. Cheng, R.W. Schefer, D.R. Willis, Thermophoresis of particles in a heated boundary layer, *J. Fluid Mech.* 101 (4) (1980) 737–758.
- [16] C.-T. Chen, Thermal instability in natural convection flow over a boundary layer subject to external electrical and magnetic fields, *Heat Mass Transfer* 45 (12) (2009) 1589–1596.
- [17] J.-Y. Jang, K.-N. Lie, Effects of blowing/suction on vortex instability of horizontal free convection flows, *AIAA J. Thermophys. Heat Transfer* 7 (4) (1993) 749–751.
- [18] M.-H. Lin, Numerical study of formation of longitudinal vortices in natural convection flow over horizontal and inclined surfaces, *Int. J. Heat Mass Transfer* 44 (9) (2001) 1759–1766.
- [19] K.C. Cheng, Y.W. Kim, Flow visualization studies on vortex instability of natural convection flow over horizontal and slightly inclined constant-temperature plates, *J. Heat Transfer* 110 (3) (1988) 608–615.
- [20] A.V. Boiko, A.V. Dovgal, G.R. Grek, V.V. Kozlov, *Physics of Transitional Shear Flows: Instability and Laminar-Turbulent Transition in Incompressible Near-Wall Shear Layers*, Springer, Berlin, 2012.
- [21] J.-S. Leu, J.-Y. Jang, Effect of a magnetic field on vortex instability of natural convection flow over a horizontal plate with blowing and suction, *J. Chin. Inst. Eng.* 31 (5) (2008) 879–884.